Impact and Tribological Characteristics of *In-Situ* 3D-Printed Glass Fibre-Reinforced PLA

Khairul Izwan Ismail[1,2], Suganti Ramarad[1], Rehan Ahmed[3] and Tze Chuen Yap[1,*]

[1]School of Engineering and Physical Sciences, Heriot-Watt University Malaysia, No 1, Jalan Venna P5/2, Precinct 5, 62200 Putrajaya, Malaysia

[2]Department of Aeronautics and Aviation Engineering, National Defence University of Malaysia, Kem Perdana Sungai Besi, 57000 Kuala Lumpur, Malaysia

[3]School of Engineering and Physical Sciences, Heriot-Watt University, Edinburgh EH14 4AS, UK

Abstract: The increasing demand for high-performance materials has led to research aimed at improving the mechanical and tribological properties of 3D-printed polymers. *In-Situ* reinforcement, where short fibres are placed between layers during printing, offers potential solutions to issues like interlayer adhesion and voids. This study explores the impact and tribological performance of glass fibre-reinforced polylactic acid (GF-PLA) composites. In the current work, glass fibre (GF) was added in situ between polylactic acid (PLA) layers during printing, whereas most previous studies used a pre-made GF-PLA composite filament. Impact strength peaked at 8.275 kJ/m² with 2.39 wt% GF but dropped with higher fibre content due to poor inter-layer adhesion. Tribological results showed a rise in the coefficient of friction (COF) with up to 2.39 wt% GF, but decreased at 4.98 wt% as the GF-PLA transfer film reduced friction. Wear tests revealed a 52% reduction in wear rate at 2.39 wt%, though wear decreased by only 24% at 4.98 wt% due to delamination. Frictional heat caused PLA softening, while harder GF led to abrasive wear, deepening wear scars at the higher fibre content.

Keywords: Fibre reinforced polymer composite, Additive manufacturing, Mechanical properties, Friction and wear.

1. INTRODUCTION

Material extrusion, also known as fused filament fabrication (FFF), is one of the techniques used in additive manufacturing (AM), also referred to as fused deposition modelling (FDM). Generally, material extrusion allows the build-up of a printed part, layer by layer, by depositing thermoplastic material through a nozzle. This technique enables the manufacture of complex shapes with a degree of design freedom that is unachievable with conventional manufacturing methods. However, the mechanical properties of FFF-printed thermoplastic parts are lower than those of injection-moulded thermoplastic parts [1].

The strength of FFF-printed parts mainly depends on the thermo-mechanical properties of materials and layer-to-layer adhesion between deposited filaments. The interlaminar bond can be divided into two types: inter-layer and intra-layer bonds. Voids within interlaminar bonds can significantly degrade the mechanical properties of the FFF-printed parts. The presence of voids is not unique to FFF-printed parts due to the nature of AM. Voids formed during the FFF printing can be classified based on their mechanism of formation into five categories: i) raster gap voids, ii) partial neck-growth voids, iii) sub-perimeter voids, iv) intra-bead voids and v) infill voids [1]. The strength of parts produced through FFF using pure thermoplastics is insufficient during mechanical tests. This limitation restricts the range of applications where FFF technology can be applied. To overcome this challenge, researchers have explored various approaches to enhance the strength characteristics of pure thermoplastics. These approaches include fibre reinforcements, particles, compatibilisers, nano-materials, etc. Among these methods, fibre-reinforced polymer (FRP) has gained significant popularity in published literature [1, 2]. Combining different materials to achieve desired mechanical and functional properties offers a promising solution to address these limitations. Consequently, there has been a growing interest in developing composite materials compatible with existing printers in recent years. Progress has been made in developing new printable composite materials reinforced with fibres, particles, or nanomaterials [2].

Reinforcement materials such as nanomaterials, particles, and fibres are usually added to FFF thermoplastics to enhance the mechanical properties and improve the performance and functionality of the printed parts. However, current fibre embedding methods may reduce the size of voids but not completely remove them. The following types of voids contribute to lowering the structural integrity of the reinforced FFF-parts: (a) micro-voids, which form within the fibre and matrix filament before printing (in between the fibres in a tow), (b) meso-voids, which form between fibre bundles (continuous fibre) after printing

*Address correspondence to this author at the School of Engineering and Physical Sciences, Heriot-Watt University Malaysia, No 1, Jalan Venna P5/2, Precinct 5, Putrajaya 62200, Malaysia; E-mail: t.yap@hw.ac.uk

Received on 05-06-2026 Accepted on 28-07-2026 Published on 05-08-2026

E-ISSN: 2311-8717/26

within a layer, and (c) macro-voids, which form between adjacent layers [3, 4].

Glass fibre, consisting of numerous fine glass fibres, is widely recognised as the most common reinforcing material for polymer matrix composites [5]. When blended with polymers, the resulting material is known as glass fibre-reinforced plastic (GFRP) or fibreglass. The combination of glass fibres, which are strong in tension, yields a composite material with relatively higher tensile and compressive strength. Parandoush *et al*. [6] employed laser-assisted bonding and laser-cutting techniques to fabricate objects using continuous glass fibre-polypropylene prepreg composites. The results demonstrated a significant increase in peel strength and lap shear strength compared to traditional methods such as hot compaction and compression moulding. In another study conducted by Chung *et al*. [7], a composite material was fabricated using Nylon-11 as the matrix material and glass beads as the reinforcement via selective laser sintering (SLS). The research encompassed theoretical modelling, numerical analysis, and experimental investigation of the composite material. They identified the optimal processing parameters to obtain the best SLS-fabricated Nylon-11.

The mechanical properties of GFRP can be enhanced through the incorporation of either short fibre or continuous fibre. Short glass fibre (SGF) composites offer versatility and can be tailored to the required tribo-mechanical properties. They can be efficiently produced using conventional plastic processing techniques such as extrusion and injection moulding. These reinforcing fillers are available in milled or chopped configurations, typically featuring diameters ranging from 10 to 20 µm [8]. Chopped fibres possess lengths typically falling within the range of 3.0 to 4.5 mm or even longer [9]. While they are recognised for their substantial reinforcement of tensile and flexural modulus [10, 11], their longer length poses challenges like nozzle clogging [12].

On the other hand, milled fibres exhibit a broader range of particle lengths, with average lengths spanning from 80 to 500 µm [13, 14]. They do not provide the same level of reinforcement as chopped fibres. However, these prolate fillers (aspect ratio, $p>1$) combine mechanical reinforcement with relatively high aspect ratios, typically ranging from 10 to 50. This differentiates them from conventional micro-sized reinforcement fillers like talc, calcium carbonate, and clays. As a result, they occupy an intermediate position between chopped fibres and traditional filler reinforcement.

Begum *et al*. [15] conducted a study on the effect of infill densities and raster angle of GF-PLA to the impact strength. The impact strength of GF-PLA specimens manufactured using FFF was investigated by varying raster angles (0°, 45°, and 90°) and infill densities (40%, 50%, and 60%) with a hexagonal infill pattern. The findings indicate that specimens printed with a 90° raster angle and 60% infill density exhibited the highest impact strength (27.8 J/m), while the lowest values were observed at a 0° raster angle. Overall, impact strength increased with increasing infill density, attributed to the greater internal structural support provided by higher infill levels. A higher infill density increases energy absorption capacity by creating a more compact internal structure capable of efficiently deforming and redistributing impact loads [16]. Karad *et al*. [17] SEM images of the fractured impact specimens printed with a 60% infill density and a 0° raster angle reveal evident rupture and interlayer debonding.

Friction and wear behaviour of FFF-printed parts was reported by Roy *et al*. [18]. They investigated the effects of layer thickness, infill pattern, raster angle, and build orientation on PLA and ABS specimens. This work used a block-on-roller tribometer under dry conditions at a rotational speed of 300 rpm, with a normal load of 25 N and 600-sec test durations. Based on their study, PLA and ABS did not differ much in terms of tribological properties under similar printing conditions. However, the result showed that the wear rate increased at higher layer thickness, infill density, and 90° raster angle, when the printing direction is perpendicular to the motion of the force. They also reported that the wear rate decreased as the infill pattern was doubled.

Perepelkina *et al*. [19] also investigated the effects of infill density on friction and wear behaviour. PLA specimens were printed with 75% and 100% infill density and tested using a plate-on-plate tribometer configuration under dry conditions at 300 rpm rotational speed and 500 N normal load for 90-sec test durations. Based on the friction versus time result, a specimen with 100% infill density changed smoothly from running-in to steady-state condition due to a more regular (even) surface compared to 75% infill. They suggested that 100% filling of printed parts is more suitable for tribological applications due to lower porosity.

Continuous fibre reinforcement has also been extensively investigated because it provides substantially higher mechanical performance than short fibre composites. Nevertheless, continuous fibre printing presents several practical limitations, including high equipment cost, complex process control, restricted printing paths and limited capability for fabricating geometrically complex components. In addition, continuous fibres cannot always be placed selectively at locations where reinforcements are most beneficial without significantly increasing manufacturing complexity. Consequently, there remains a need for alternative reinforcement strategies that retain the simplicity of conventional FFF while providing targeted reinforcement at critical structural regions.

Although studies have shown that adding reinforcement can improve the mechanical properties of 3D-printed polymers, the mechanical properties of 3D-printed polymer composites are still weaker than those of polymers produced by traditional moulding methods [20]. There are three primary methods for embedding fibres in the manufacture of FFF-printed fibre-reinforced polymer composites [1]: embedding before the printing process (M1), embedding within the nozzle (M2), and embedding directly into the component during printing (M3). Traditional FFF-printed short-fibre composites were reinforced before printing. This approach does not strengthen the weakest region. The area between the layers where voids occur. Therefore, FFF-printed composites made from polymer filament reinforced with either particles, fibres, nanocomposites (M1-pre-reinforced filament) and embedding within the nozzle (M2) may not be the most effective solution to address this problem.

Despite the extensive research on fibre-reinforced FFF composites, most existing studies have focused on improving the properties of the filament itself by incorporating fibres before extrusion. Comparatively few studies have investigated reinforcement strategies that directly target the interlayer interface, where insufficient polymer diffusion, weak neck growth and void formation predominantly govern the mechanical performance of FFF components. Therefore, an effective reinforcement technique that specifically strengthens the interlayer region while maintaining process simplicity remains an important research challenge. The recently developed in-situ fibre dosing approach offers a promising alternative by introducing short glass fibres directly between successive deposited layers, thereby reinforcing the weakest region of the printed structure rather than uniformly reinforcing the entire filament.

Previous research has shown the potential of an *in-situ* fibre polymer composite (M3), but the composites were fabricated manually [21-23]. *In-situ* reinforcement during printing is a possible method to improve the mechanical properties of 3D-printed parts further. An *in-situ* short-fibre reinforcement method was proposed recently [24]. The *in-situ* 3D-printed PLA composites improved tensile behaviour [25]. The short fibre is placed between the layers and also fills the voids. Therefore, the *in-situ* short fibre reinforcement method can potentially address the interlayer adhesion and voids problem mentioned earlier. In the current study, the impact properties of FFF-printed GF-reinforced PLA (GF-PLA) composites were evaluated. The tribological behaviour of FFF-printed GF- PLA against steel was also investigated.

Unlike commercially available GF-PLA filaments, where short glass fibres are compounded into the filament prior to printing, the proposed in-situ reinforcement strategy introduces the glass fibres directly between successive deposited PLA layers during the FFF process. This approach specifically targets the weakest region of FFF components, the interlayer interface, where poor bonding and void formation commonly initiate failure. By positioning the reinforcement at the interlayer region instead of distributing it uniformly throughout the filament, the proposed technique offers a different reinforcement mechanism that has the potential to improve interlayer bonding while avoiding several limitations associated with pre-compounded composite filaments, such as fibre breakage during extrusion, nozzle clogging and restricted control over fibre placement.

2. MATERIALS AND METHODS

2.1. Fabrication of the in-situ GF-PLA Composites

The PLA filaments utilised in this study were sourced from Forcemaker3D (Nazca Scientific Sdn. Bhd., Cheras, Malaysia), while the milled E-glass fibre variant was provided by Shenzhen Feige Composite Fibre Co., Ltd., located in Shenzhen, China. The milled E-glass fibre was generated from E-glass strands

Table 1: Specification of Glass Fibre (manufacturer data)

Specifications	Average Value
Model	MEF-13-100
Colour	White
Glass type	E-glass
Mesh	100
Fibre diameter	13 microns
Fibre length	160 microns
Aspect ratio	12:1
Bulk density	0.67 g/cc
Moisture content	<1.5%
Loss of ignition	<1%
Alkali content/R2O (%)	<0.80
Sizing	Silane
Contamination	Free from dirt, lumps, and unmilled fibre

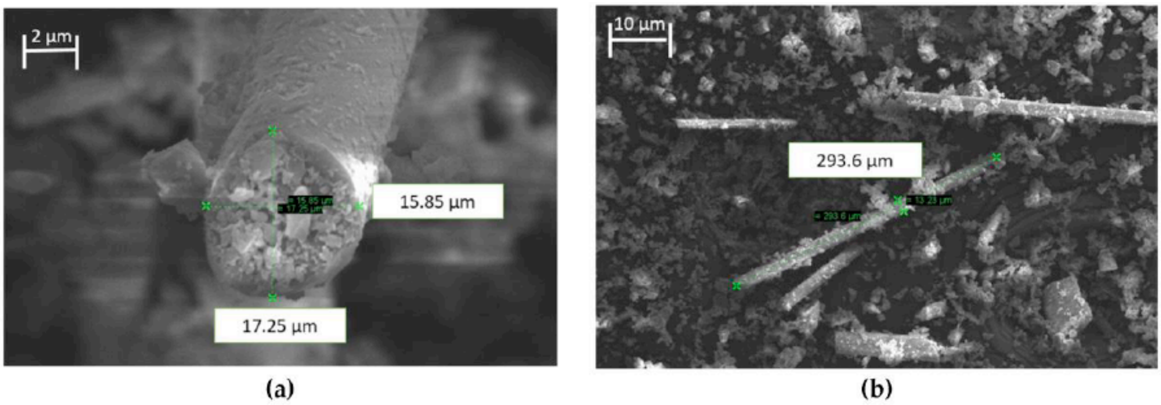

Figure 1: SEM image of the GF: (**a**) fibre diameter, and (**b**) fibre length [25].

subjected to chopping through a ball mill, followed by wet grinding, drying, and screening. These procedures are commonly employed to reinforce unsaturated, epoxy, and phenolic resins. Table **1** outlines the specifications of the GF used in this study. Based on the datasheet provided by the supplier, milled GF was treated with organic silane as a coupling agent to improve the interaction between GF and PLA. The scanning electron microscopy (SEM) images of the milled GF with an average fibre diameter of 13 µm and fibre length of 160 µm (Table **2**) used in this research work are shown in Figure **1**.

2.2. In-Situ GF-PLA Samples Fabrication

FFF 3D printing was conducted using a Forcemaker3D S220 printer, with a nozzle diameter of 0.4 mm, printing speed of 60 mm/s, layer thickness of 0.2 mm, infill density of 100%, and alternating deposition directions for the fill pattern between 45° and 135° for different layers. The standard printing parameters utilised in this research are outlined in Table **2**. The procedure involved depositing molten PLA onto the print bed or parts through the original nozzle, followed by dosing GF onto the molten PLA using the supplementary dosing unit. The details of the composite fabrication process were reported in a previous study, and a schematic diagram of the process is shown in Figure **2**. Short GF-reinforced PLA (GFPLA) samples featuring varied fibre contents were fabricated employing distinct fibre deposition rates of 200, 235 and 250 rpm (Table **3**). The GF content for all samples was determined using thermogravimetric analysis (TGA), as explained in previous work [24].

Table 2: Printing Parameters used in this Study

Parameter	Standard Value
Nozzle temperature (°C)	210
Heating bed temperature (°C)	70
Number of shells	3
Infill pattern Infill percentage, (%)	Rectilinear 100
Raster angle (°)	(+45/−45)
Layer thickness (mm)	0.2
Printing speed (mm/s)	60
Build orientation	Flat

It should be noted that the mechanical and tribological performance reported in this study is also influenced by the selected FFF processing parameters. The printing temperature of 210℃ was selected to provide sufficient melting of the PLA matrix while promoting polymer diffusion between adjacent deposited layers. A layer thickness of 0.2 mm was adopted to achieve a balance between printing quality

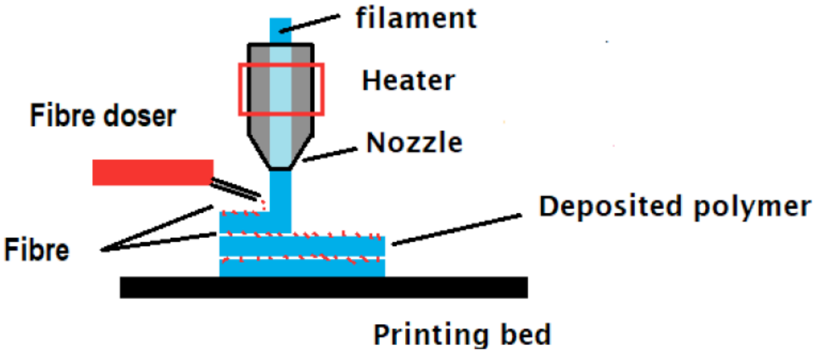

Figure 2: Fabrication of FFF-printed in-situ fibre-reinforced polymer (blue – polymer; red particles – short fibre) [24].

Table 3: GF Content of the Test Specimen [25]

Name	Motor Speed of the Fibre Doser (rpm)	Contents of Glass Fibre (mass fraction, %)
PLA	0	0
GFPLA-1	200	1.02
GFPLA-2.4	235	2.39
GFPLA-5	250	4.98

and interlayer bonding, whereas the ±45°raster orientation provided a more uniform distribution of mechanical loading during impact testing. In addition, the printing speed of 60 mm/s ensured stable fibre deposition while minimizing printing defects. Although these parameters were maintained constant to isolate the influence of glass fibre content, previous studies have shown that variations in processing conditions can significantly affect crystallinity, interlayer adhesion, void formation and wear behaviour.

The selected fibre contents (1.02, 2.39 and 4.98 wt%) were determined based on the stable operating range of the fibre dosing system developed in the previous work [25]. These reinforcement levels also represents low, intermediate and high fibre loading conditions while maintaining continuous printing without excessive fibre accumulation of nozzle interference. Higher fibre contents were not considered because preliminary observations indicates unstable fibre deposition and deterioration of interlayer bonding.

All specimens for impact strength and tribological tests were fabricated according to ASTM D6110-04 and ASTM G99-17, respectively. These specimens were designed using computer-aided design (CAD) CATIA V5 software. Then, the designs were sliced into an open-source slicer's software called Cura and then transformed into STL files for printing.

2.3. Impact Test

The Charpy impact tests were performed to investigate the energy absorption of the PLA composite with respect to the different GF content. Energy loss by the pendulum during the breakage of the specimen is the sum of the energy required to initiate and propagate the fracture of the specimen. Notched specimens 80 mm long, 10 mm wide and 8 mm thick with a notch size of 2.54 mm were fabricated according to ASTM D6110 and tested using a pendulum impact tester (ZwickRoell, Ulm, Germany). Five tests were performed for each GF-PLA composite, and average values with standard deviation are reported. Impact strength for each specimen was calculated using the equation:

$$\sigma_i = \frac{E_i}{w \times t}$$

Where,

σ_i = impact strength in kJ/m^2,

E_i = energy absorbed by the composite in kJ,

w = width of the specimen in m and

t = thickness of the specimen in m.

2.4. Tribological Test

A pin-on-disc apparatus was used to evaluate the GF-PLA composites' friction and wear properties per the ASTM G99-17 standard. The pins, measuring 8 x 8 x 48 mm and with a 90° print orientation, were FFF-printed. The counter face was an ASSAB 760 steel disc with a hardness of 34 HRC. The radius of the wear track is 34 mm. The test duration was 45 minutes with a 300 rpm disc's rotational speed, a normal load of 12.5 N, and a 2,884 m sliding distance. Figure **3** below shows the pin-on-disc setup for the tribological test. Before the tribological test initiate, the initial weight of each pin was measured and recorded using an electronic balance with an accuracy of 0.001 g (A&D FZ -500i, A&D company, Tokyo, Japan). The disc surface was cleaned sequentially with abrasive papers of ascending grit sizes. Subsequently, it was cleaned using a cloth soaked in acetone for three minutes. The surface of the disc was then dried in room temperature.

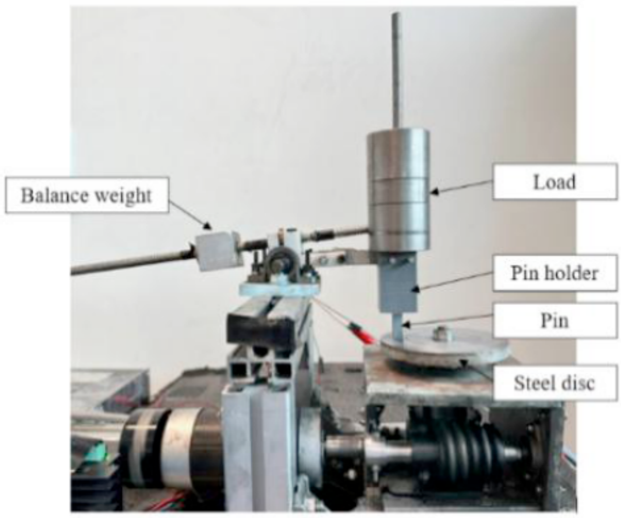

Figure 3: Tribotester rig.

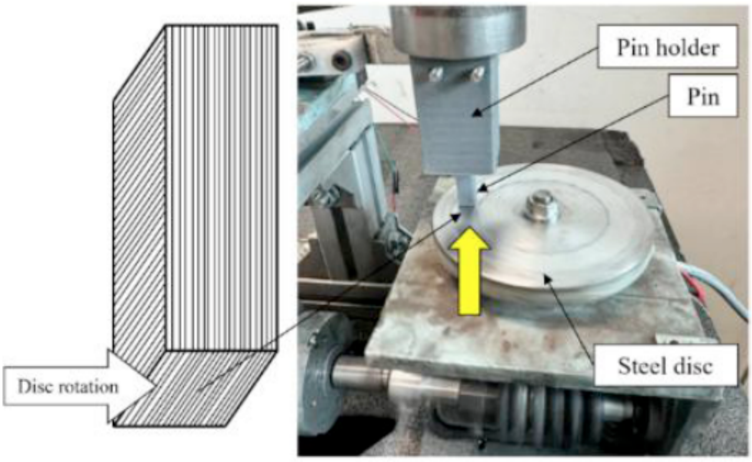

Figure 4: Friction and wear experiment.

Figure **4** depicts the position of the pin (specimen) during the tribological test. A load of 12.5 N was applied to the guiding rod to serve as the normal force for the test. The pin was secured in the pin holder, and the tribotester's disc was then allowed to rotate by adjusting the speed knob. The disc's rotational speed was recorded using a tachometer (CT6/LSR Optical-Contact Handheld tachometer, Compact Instruments Ltd, Lancashire, BL3 2AB, United Kingdom). The frictional force experienced by the pin was measured by a load cell and shown as an output voltage on the connected multimeter. The pin was removed at the end of the test, and its weight was again measured using the electronic balance to calculate the mass loss during the wear test. This process was repeated three times using identical pins at the same load and disc rotation speed, and averaged values are reported. The steady-state friction force value was used to calculate the coefficient of friction (COF). Friction and wear data were analyses to establish a relationship with GF content.

3. RESULTS AND DISCUSSION

3.1. Impact Strength

Figure **5** shows the impact strength of neat PLA and GF-PLA composites. The FFF-printed neat PLA has an impact strength of 1.775 kJ/m^2, which is lower than the previously published results. Hasan *et al*. [26] compared the impact strength of FFF-printed recycled PLA with the impact strength of new PLA, printed at three different layer heights (0.1, 0.2, 0.3 mm), three different infill percentages (60%, 80%, 100%) and different printing temperatures (195°C, 205°C, 215°C). Their results showed that the impact strengths of the new PLA ranged from 3.8 kJ/m^2 to 5.4 kJ/m^2, depending on the infill percentage, layer height, and printing temperature. In another work, Slapnik *et al*. [27] showed that the impact strength of 3D-printed PLA printed at 230°C, with a layer height of 0.3 mm and 20% infill density, was 10.44 kJ/m^{2,} whereas the injection-moulded PLA was 12.9 kJ/m^2. The difference in these values was caused by the different printing parameters used in the tests.

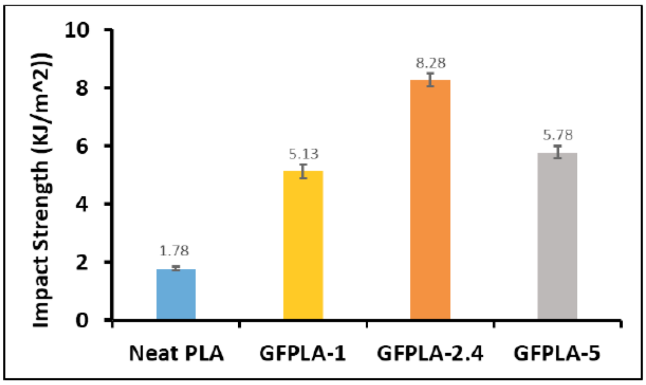

Figure 5: Impact strength of neat PLA and GFPLA composites.

When the 1.02 wt% GF is added to the PLA matrix using the *in-situ* method, the impact strength of the GF-PLA laminate composite increases to 5.125 kJ/m^2. The GF-PLA composites showed an increment of impact strength up to 2.39 wt% GF, followed by a decrease as the GF concentration in the PLA matrix increased to 4.98 wt%. The current study showed that initially, the neat PLA had an impact strength of 1.775 kJ/m^2, but after adding GF, the impact strength of GFPLA-1 and GFPLA-2.4 increased to 5.125 kJ/m^2 and 8.275 kJ/m^2, respectively, translated to increases of 188.7% and 366.2% impact strength. However, after 2.39 wt% GF, a decline in impact strength was observed for the GFPLA-5 composite. This was due to flaws in the GFPLA-5 composite, resulting in a brittle fracture behaviour during impact. Milled E-glass fibre has a significantly lower thermal conductivity (0.03 $Wm^{-1}K^{-1}$) compared to PLA (0.185 $Wm^{-1}K^{-1}$)[31]. Thus, materials with lower thermal conductivity transfer heat at a slower rate, including a relatively large amount of GF on the surface of hot extruded PLA, reduces the surface temperature of the PLA by drawing heat away from it.

Although the incorporation of glass fibre significantly improved the impact strength up to 2.39 wt%, a noticeable reduction was observed when the fibre content increased to 4.98 wt%. This behaviour can be attributed to the deterioration of the interlayer bonding mechanism caused by excessive fibre deposition. Unlike neat PLA, where intimate contact between adjacent layers promotes polymer diffusion and neck growth, the accumulation of a relatively large amount of glass fiber possesses a substantially lower thermal conductivity than PLA. Consequently, heat transfer from the newly deposited molten PLA layer to the previously deposited layer is restricted, reducing the temperature available for molecular diffusion across the interface. Insufficient polymer diffusion limits neck growth between adjacent layers, resulting in weaker interlayer adhesion and increasing the susceptibility of the printed composites to interlayer delamination during impact loading [25].

On the other hand, since milled E-glass fibres are not present between adjacent layers within the same layer, heat transfer between these layers can occur more effectively, enhancing the intralayer bonds, as shown in Figure **6**. Previous studies have shown that GFPLA-5 has fewer voids compared to the neat PLA, GFPLA-1, and GFPLA-2.4, as shown in Figure **7**. Reduced voids within the GFPLA-5 composite deteriorate the capability of the composite to absorb impact energy. When a composite material is subjected to impact, the presence of voids can contribute to energy absorption. These processes help dissipate the impact energy, preventing it from being transferred directly to the composite structure, which can reduce the likelihood of catastrophic failure [28-30]. In the case of the GFPLA-5 composite, the decrease in voids means there are fewer sites within the material to facilitate these energy-dissipating mechanisms. Without these voids, the composite becomes more rigid and less capable of deforming plastically to absorb energy. Instead, the impact energy is more likely to be concentrated and transferred through the material, leading to brittle fracture. Therefore, while minimising voids can enhance mechanical properties like tensile strength, it can negatively affect the FFF-printed PLA's ability to absorb and dissipate impact energy, reducing impact strength.

The deterioration of the interlayer bonding directly influences the impact failure mechanism. During impact loading, the absorbed energy is primarily dissipated through plastic deformation and crack propagation across adjacent deposited layers. In the optimally reinforced composite (2.39 wt% GF), adequate interlayer bonding enables efficient load transfer between layer while allowing the composite to absorb impact energy before fracture. However, at higher fibre contents, the weakened interlayer interface becomes the preferred crack propagation path. Instead of being dissipated through progressive deformation, the impact energy is rapidly released through interlayer

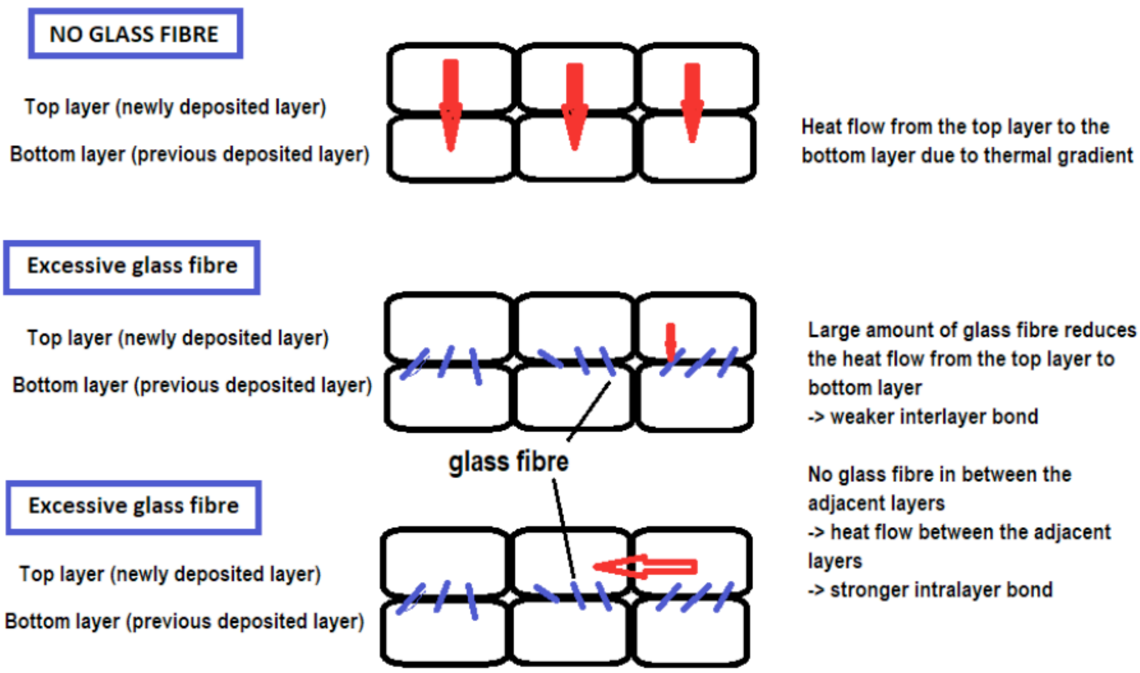

Figure 6: The effect of *in-situ* GF on the interlayer and intralayer bonds.

delamination, resulting in brittle fracture and a reduction in impact strength. This proposed failure mechanism is consistent with the tensile behaviour reported in our previous study [25], where excessive in-situ glass fiber reinforcement reduced interlayer adhesion because of insufficient heat transfer between deposited layers.

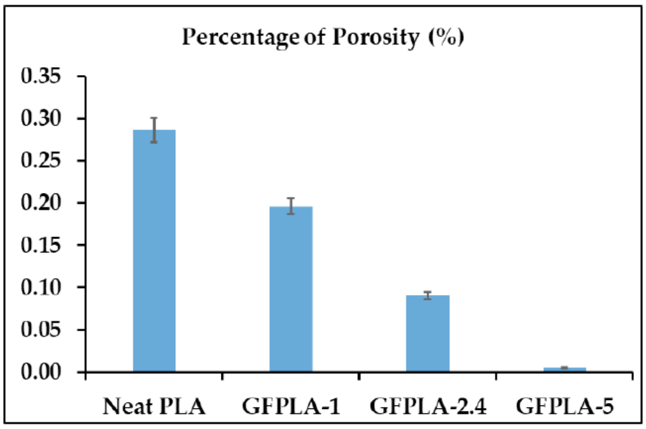

Figure 7: The percentage of porosity with respect to GF content [25].

In summary, adding GF to the PLA matrix enhances the impact strength. Similar trends have been observed in other polymer composites, such as core-shell rubber/PLA [27], aliphatic polyester/PLA [27], GF-reinforced ABS [32], and Basalt fibre-reinforced PLA [33]. However, excessive reinforcement created a negative impact, similar to a recent work.

The proposed mechanism is further supported by Figures **6** and **7**. Figure **6** schematically illustrates how excessive glass fibre located at the interlayer interface interrupts heat transfer between adjacent deposited layers, thereby restricting neck growth and reducing interlayer bonding strength. Previous tensile investigations demonstrated that this reduction in interlayer heat transfer resulted in lower interlayer adhesion in specimens containing excessive glass fibre. In addition, Figure **7** shows that increasing fibre content reduces the overall porosity of the printed composites. Although lower porosity generallly improves stiffness and tensile properties, it also decreases the number of local deformation sites available for dissipating impact energy.Consequntly, the GFPLA-5 composite become more rigid and less capable of absorbing impact energy, causing fracture to occur through brittle interlayer delamination rather than stable crack propagation.

Therefore, the reduction in impact strength at higher glass fibre contents is not caused by the presence of glass fibre itself but by the excessive accumulation of reinforcement at the interlayer interface, which alters the thermal history during deposition and weakens the interlayer bonding mechanism. These findings indicate that the mechanical performance of in-situ reinforced FFF composites is governed by an optimum balance between fibre reinforcement and interlayer polymer diffusion, whereas excessive fibre loading promotes premature interlayer delamination and brittle failure under impact loading.

3.2. Tribological Properties

Tribological performance is governed by the interaction between friction, wear and surface damage occurring at the contact interface during sliding. For fibre-reinforced polymer composites fabricated by FFF, the wear behaviour is influenced not only by the intrinsic properties of the reinforcing fibres but also by the quality of interlayer bonding, fibre–matrix adhesion and the formation of wear debris during sliding. Therefore, a comprehensive tribological assessment should consider the coefficient of friction (COF), wear rate and worn surface morphology collectively rather than as independent observations.

In the present study, the incorporation of an appropriate amount of in-situ glass fibre significantly enhanced the tribological performance of the printed PLA composites. At the optimum fibre content (2.39 wt%), the deposited glass fibres effectively reinforced the interlayer region while maintaining adequate polymer diffusion between adjacent deposited layers during printing. This improved the interlayer integrity, promoted more efficient load transfer during sliding and reduced local plastic deformation, resulting in lower wear rates and stable friction behaviour.

In contrast, increasing the glass fibre content to 4.98 wt% resulted in deterioration of the tribological performance. Excessive fibre deposition restricted heat transfer during deposition, thereby reducing polymer diffusion and weakening the interlayer bonding. Under sliding conditions, these weak interfaces promoted interlayer delamination and fibre debonding. Detached glass fibres subsequently acted as hard third-body abrasive particles trapped between the PLA specimen and the steel counter face, accelerating surface damage and material removal.

The proposed wear mechanism is strongly supported by the SEM observations of the worn surfaces. Specimens containing moderate glass fibre reinforcement exhibited relatively smooth wear tracks with shallow grooves and limited fibre pull-out, indicating mild abrasive wear. Conversely, the specimen containing 4.98 wt% glass fibre exhibited severe surface damage characterised by deep grooves, interlayer delamination and extensive fibre pull-out. These morphological observations are consistent with the measured friction and wear results, confirming that optimum tribological performance is governed by the balance between effective fibre reinforcement and adequate interlayer bonding.

3.2.1. Coefficient of Friction (COF)

The impact of GF reinforcement on the COF of FFF-printed PLA is depicted in Figure **8**. Adding 1.02 wt% GF to the PLA increased the FFF-printed GF-PLA composite COF to 0.34, compared to 0.32 of neat PLA. When GF content increased to 2.39 wt% (GFPLA-2.4), the average COF increased to 0.35. The increase of COF with the increase in fibre content was due to the higher friction force required to shear the adhesion junctions formed on the surface as more fibre is embedded in the matrix materials, as reported [34]. However, at the highest GF content, which is 4.98 wt% (GFPLA-5), there was a noticeable drop in COF, even lower than that of neat PLA. A similar trend in COF was observed when GF was used to reinforce polypropylene [35], where the COF increased with the inclusion of GF, reached a maximum and then decreased. This phenomenon can be ascribed to the formation of a PLA film blended with GF particles on the contact surface of the steel disc, as illustrated in Figure **9**. The material underwent a softening effect with the rise in temperature between the specimen and the counter surface due to friction. As observed previously in the tensile properties, an excessive amount of GF led to weak inter-layer bonds, causing delamination and detachment of the GF from the PLA specimen [25]. During the wear tests, continuous sliding leads to high temperatures, which cause delamination and fibre detachment, resulting in decreased COF.

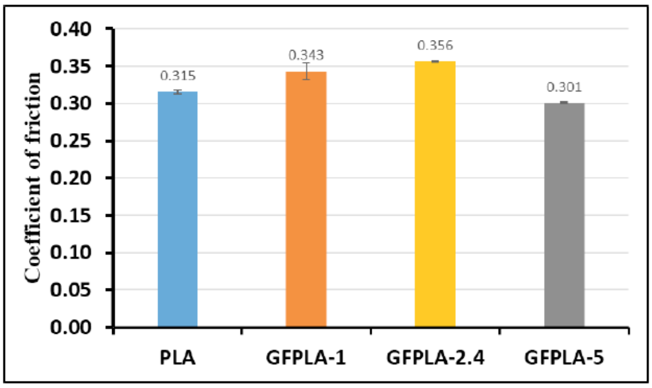

Figure 8: COF versus GF content.

Additionally, for the 4.98 wt% (GFPLA-5), the COF decreases due to the smooth transfer of a thin PLA film during sliding and with the presence of GF (wear debris), which reduces the frictional force, *i.e*. the sliding pair was changed from PLA-steel to PLA-PLA/GF. The sliding mechanism was changed from pure sliding to sliding-rolling due to the presence of GF as a third body. The wear debris detached from the PLA pin consists of PLA and GF debris. Some of the wear debris was trapped between the PLA pin and the steel disc and formed a third body. The soft PLA debris is deformed and reattached to the PLA pin or/and the steel disc, whereas the hard GF is either rolled freely between the PLA pin/steel interface (rolling friction) or embedded into the PLA pin, causing abrasive friction.

Figure 9: Formation of thin PLA film on the contact surface.

3.2.2. Wear Rate

The wear rate, measured in kilograms per meter (kg/m), indicates mass loss over a specific distance and remains unaffected by the applied load. On the other hand, the specific wear rate, measured in kilograms per Newton meter (kg/Nm), varies with the load applied to induce wear, representing the mass loss per meter per unit load. Wear rate is critical for evaluating and comparing material wear performance, influenced by factors such as sliding distance, applied normal load, and material hardness. Since the parameters of wear testing remain constant during sliding, the wear performance of the GFPLA composite is primarily influenced by the contents of the GF. Figure **10** illustrates that GFPLA composite specimens exhibit lower wear than neat PLA specimens. The wear of the material decreases with an increase in GF content. Specifically, the wear rate of GFPLA composites decreased by approximately 52% when GF content was increased to 1.02 wt% (4.16×10^{-9} kg/m) and 2.39 wt% (4.16×10^{-9} kg/m), whereas it decreased by only 24% when the GF content rises to 4.98 wt% (6.59×10^{-9} kg/m). This indicates that GF reinforcement reduces the wear rate of printed PLA significantly. The compressive stress based on the apparent contact area from the pin dimensions was 0.195 MPa. The actual stress will be higher as the real contact area will be lower due to surface texture and porosity in the print.

For an average friction coefficient of 0.3 under a normal load of 12.5 N, the friction force at the contact will be 3.75 N. The combined effect of compressive stress (0.195 MPa) and shear force due to friction will yield a shear stress of 0.112 MPa within the contact region as a lower bound estimate. This stress can increase by orders of magnitude as the real contact area decreases.

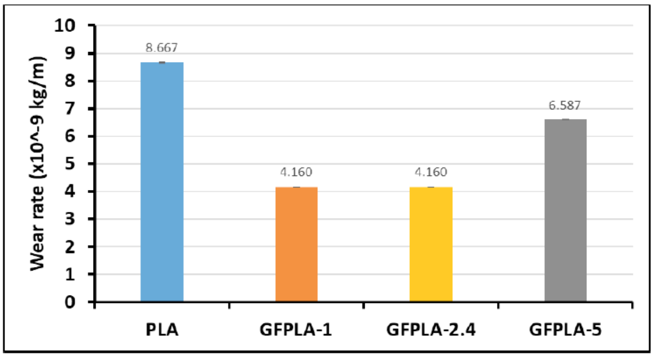

Figure 10: Wear rate of the FFF printed PLA and PLA composites.

Previous investigations reported that the interlayer shear strength of the FFF parts varies from 6.1 MPa to 15 MPa [36, 37]. The interlayer shear strength of FFF prints depends on several factors, such as the infill pattern, printing sequence, layer height, printing line width, etc. [36-38]. Furthermore, various testing methods have been used to determine the interlayer shear strength, as currently, there is no standardised procedure for determining the interlayer shear strength for FFF-printed parts [36].

Wear loss decreased for GFPLA-1 and GFPLA-2.4 due to stronger layer adhesion between GF and PLA, resulting in better wear resistance. However, when the GF content increased to 4.98 wt% (GFPLA-5), layer adhesion deteriorated due to the excess amount of GF. This has been reported in previous work [25], in which an excess amount of GF decreases the surface temperature of PLA, thereby reducing the heat transfer between layers, which is necessary to form a strong bond between the newly deposited layer and the previously deposited or bottom PLA layer. As a result, delamination occurred within the composite layer [25]. A similar observation was reported by Chand *et al*. for short glass fibre polyester composites produced by the hand lay-up method [39]. They reported that the wear volume of their composite decreased as the GF content increased from 40% to 45% due to the higher energy required to facilitate failure in GF. It is important to note that their composite was not fabricated using the FFF method. An excessive amount of glass fibre powder acts as a barrier, hindering the necessary heat transfer for neck growth between the deposited filaments, thereby weakening the interlayer bonds [25].

Figure **11** presents the specific wear rate findings for both neat PLA and GF-PLA composites. It shows the same trend in terms of wear rate versus GF content. Compared to neat PLA specimens, GF-PLA composites demonstrate lower specific wear rates, indicating an improvement in wear resistance through GF reinforcement. This enhancement is attributed to the transfer of the applied load from the polymer matrix to the reinforced GF during the sliding process, a phenomenon contingent upon the robust interfacial adhesion between the fibre and the matrix. Adequate adhesion at the interface between the GF and PLA matrix facilitates the uniform distribution of the applied load across the fibre-matrix system, thereby enhancing the wear resistance properties of the composites. The wear resistance of GF-PLA composites escalates with GF reinforcement.

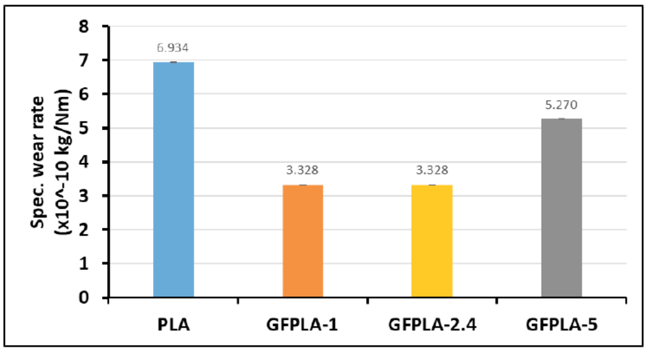

Figure 11: Specific wear rate versus GF contents.

Although the coefficient of friction decreased for the GFPLA-5 specimen, its wear rate increased considerably. This apparent contradiction indicates that friction coefficient alone is insufficient to describe tribological performance. The lower friction coefficient resulted from the formation of a transfer film together with the rolling action of detached glass fibre particles, whereas the increased wear rate originated from severe interlayer delamination, fibre pull-out and accelerated material removal. Therefore, the wear behaviour was governed primarily by the integrity of the interlayer interface rather than by the measured friction coefficient alone.

At the highest GF content, a transfer film of PLA blended with GF particles was observed on the contact surface of the steel disc, as illustrated in Figure **9**. Frictional heat is generated when two surfaces slide against each other. Milled E-glass fibre has a lower thermal conductivity than PLA, which is 0.03 $Wm^{-1}K^{-1}$, while PLA is 0.185 $Wm^{-1}K^{-1}$ [28]. PLA composite with more GF retains more heat, leading to a rise in its surface temperature. PLA is sensitive to temperature and begins to soften at elevated temperatures, leading to plastic deformation of the material. In GF-PLA composite with excessive GF content, weak interfacial adhesion between the fibres and the PLA matrix causes delamination of the bottom layer of the specimen, allowing GF to disperse onto the contact surface. The milled GF, being abrasive, becomes wear particles (three-body abrasion), which escalates the wear rate on the contact surface. Based on the result, it is suggested that an optimal content of *in-situ* fibre reinforcement improves the wear resistance of GF-PLA composites. In summary, the optimal GF content in reinforced composites has better interfacial adhesion, effectively transferring loads while minimising delamination and enhancing the material's tribological performance under sliding conditions.

3.2.3. Worn Surface Morphology

SEM micrographs of the worn surfaces provide direct evidence supporting the proposed tribological wear mechanism. The wear morphology changes progressively with increasing glass fibre content and closely correlates with the measured coefficient of friction and wear rate. At lower fibre contents, the worn surfaces exhibited relatively smooth wear tracks with shallow grooves, indicating limited material removal and mild abrasive wear. These observations are consistent with the lower wear rates measured for GFPLA-1 and GFPLA-2.4, suggesting that adequate interlayer bonding effectively restricted crack propagation and fibre pull-out during sliding.

PLA is a softer material compared to steel. When PLA slides against hard steel, frictional heat is generated. When the sliding duration increases, more frictional heat is generated, and in consequence, the hardness of the PLA pin is reduced, and the melt flow rate of PLA increases. Milled GF is harder and has higher melting temperatures compared to PLA. As friction heat between contact surfaces rises during the tribo-test, it causes material softening and material transfer from the PLA pin to the steel disc, as shown in Figure **9**. The thin film layer is a blend of PLA with milled GF detached from the specimen, and the milled GF acts as a three-body sliding-rolling mechanism. The milled GF being abrasive caused deep wear scars on the specimen's surface. This can be seen in Figure **12**. The higher the GF content, the more severe the wear damage.

In contrast, the worn surface of the GFPLA-5 specimen exhibited severe surface damage characterised by deep grooves, extensive fibre pull-out and interlayer delamination. These morphological features indicate that excessive glass fibre deposition weakened the interlayer interface, allowing fibres to detach from the matrix during sliding. The detached fibres subsequently acted as abrasive third-body particles between the specimen and the steel disc, producing severe abrasive wear and accelerating

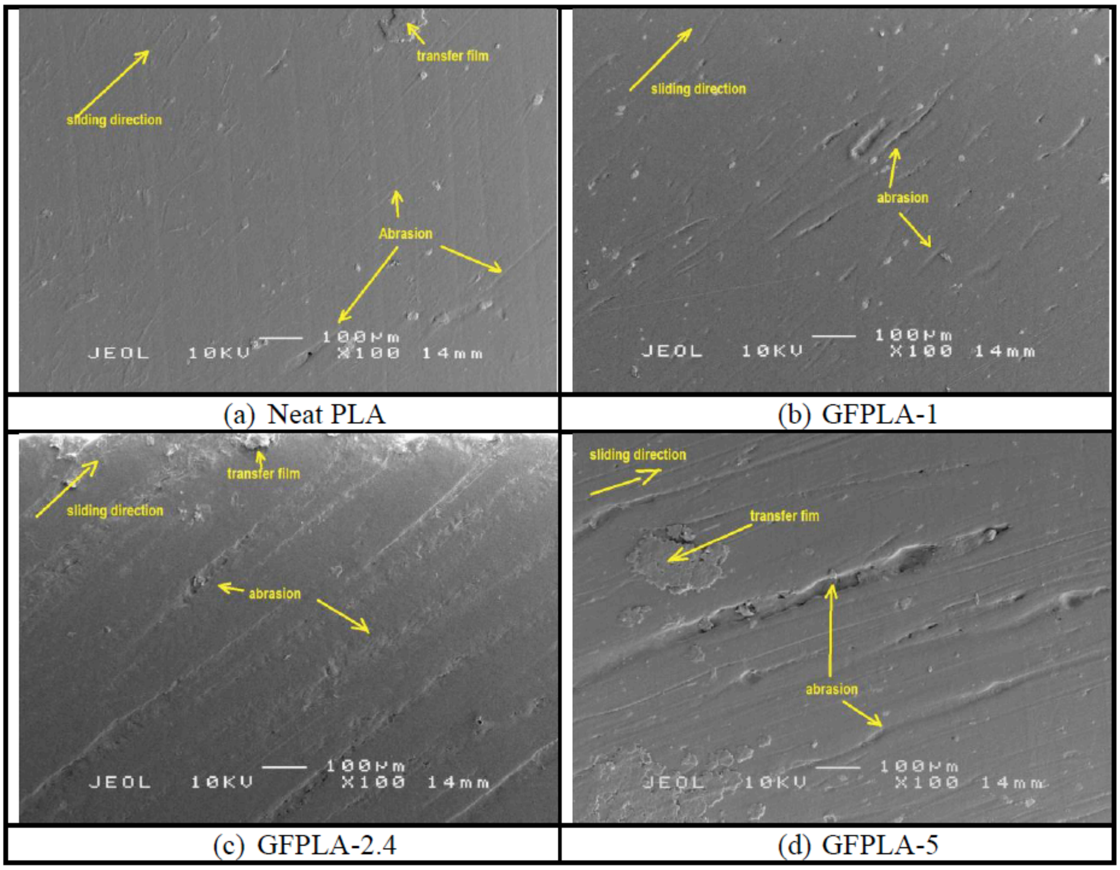

Figure 12: SEM images of worn surfaces of.

material removal. This observation explains why the GFPLA-5 specimen exhibited the highest wear rate despite having the lowest coefficient of friction.

Overall, the tribological behaviour of the in-situ glass fibre reinforced PLA composites was controlled by the interaction between fibre reinforcement, interlayer bonding and third-body abrasion. Moderate glass fibre contents improved wear resistance by strengthening the interlayer interface and promoting efficient load transfer during sliding. However, excessive fibre loading weakened interlayer bonding because of reduced polymer diffusion during deposition, resulting in fibre pull-out, interlayer delamination and the formation of abrasive wear debris. Although the transfer film and rolling glass fibre particles reduced the coefficient of friction, the accompanying increase in third-body abrasion accelerated material removal, leading to inferior tribological performance. The excellent agreement between the friction measurements, wear rate and SEM observations confirms the proposed wear mechanism.

4. CONCLUSIONS

This study demonstrates the significant impact of *in-situ* GF reinforcement on the mechanical and tribological properties of FFF-printed polylactic acid (PLA) composites. The following are the conclusions obtained from the current investigation.

1. Optimal GF content for impact strength: The incorporation of GF into PLA through *in-situ* reinforcement improved impact resistance, with impact strength peaking at 8.275 kJ/m² with 2.39 wt% GF.

2. Tribological performance of GF-PLA composites of different fibre content: Tribological testing showed that the COF initially increased with up to 2.39 wt% GF but decreased at 4.98 wt% due to the formation of a PLA-GF film that altered the friction surfaces. Wear tests showed a substantial reduction in wear rate with GF content up to 2.39 wt%, with a 52% decrease in wear rate. However, at 4.98 wt%, wear reduction was limited to 24% due to poor layer adhesion and increased wear scars.

3. Wear Mechanism: SEM analysis of worn surfaces indicated that frictional heat caused PLA softening and material transfer, with GF contributing to abrasive wear and forming a thin film on the steel disc. The presence of GF shifted the wear mechanism from sliding abrasion to sliding-rolling, highlighting their role as a third body in the tribological process. Overall, optimal fibre content is crucial, while *in-situ* GF reinforcement enhances the mechanical performance of FFF-printed GF-PLA composites. Excessive GF can impair interlayer adhesion and alter the wear mechanisms, leading to diminished performance.

These findings provide valuable insights for optimising the properties of GF-reinforced FFF-printed PLA composites for various applications.

The proposed in-situ glass fibre reinforcement technique demonstrates considerable potential for engineering applications requiring lightweight structures with enhances impact and wear performance. Compared with commercially available of GF-PLA filaments, where the reinforcement is uniformly dispersed throughout the filament during extrusion, the proposed approach introduces short glass fibres directly between successive deposited layers. This targeted reinforcement strategy strengthens the interlayer interface, which is generally recognized as the weakest region in FFF-printed components. Consequently, the proposed method offers greater flexibility in controlling fibre content and reinforcement location without requiring specially manufactured composite filaments.

Potential engineering applications include lightweight UAV airframe components, drone housings, robotic fixtures, cusomised manufacturing tooling, protectives covers, wear pads, aerospace interior components and non-critical structural parts where a balance between impact resistance, wear resistance and low weight is desirable. The proposed technique may also benefit defense-related applications, where rapid fabrication of customized replacements parts and mission-specific components is required.

This study has several limitations. The investigations were limited to a single PLA material, one glass fibre length, one printer configuration and fixed FFF processing parameters. Furthermore, tribological evaluation was performed only under dry sliding conditions at room temperature, while the influence of environmental conditions, lubrication and long-term service performance was not investigated.

Future studies should investigate the influence of diiferernt glass fibre lengths, fibre diameters, coupling agents and alternative polymer matrices on the mechanical and tribological behaviour of in-situ reinforced composites. Further optimization of raster orientation, layer thickness, printing temperature and fibre content using Design of Experiment (DOE) is also recommended. In addition, fatigue performance, environmental durability and long-term tribological behaviour should be evaluated to further establish the suitability of the proposed reinforcement technique for engineering applications.

AUTHOR CONTRIBUTIONS

Conceptualisation, T.C.Y.; methodology, K.I.I., S.R., R.A. and T.C.Y.; software, K.I.I.; validation, K.I.I, testing, K.I.I.; investigation, K.I.I., S.R. and T.C.Y.; writing—original draft preparation, K.I.I. and T.C.Y.; writing—review and editing, S.R., R.A. and T.C.Y.; supervision, S.R., R.A. and T.C.Y.; project administration, T.C.Y.; funding acquisition, T.C.Y. All authors have read and agreed to the published version of the manuscript.

ACKNOWLEDGMENTS

K.I.I. would like to thank Malaysia Ministry of Higher Education (MOHE) and Heriot-Watt University Malaysia for the financial support. T.C.Y. would like to thank the funder of this project.

CONFLICTS OF INTEREST

The authors declare no conflict of interest.

FUNDING

This work was funded by the Malaysia Ministry of Higher Education (MOHE), under Fundamental Research Grant Scheme (FRGS) grant no. FRGS/1/2019/TK03/HWUM/02/01.

REFERENCES

[1] Ismail, K.I.; Yap, T.C.; Ahmed, R. 3D-Printed Fibre-Reinforced Polymer Composites by Fused Deposition Modelling (FDM): Fibre Length and Fibre Implementation Techniques. Polymers (Basel). 2022, 14. https://doi.org/10.3390/polym14214659

[2] Hofstätter, T.; Pedersen, D.B.; Tosello, G.; Hansen, H.N. State-of-the-Art of Fibre-Reinforced Polymers in Additive Manufacturing Technologies. 2017, 36, 1061-1073. https://doi.org/10.1177/0731684417695648

[3] Mehdikhani, M.; Gorbatikh, L.; Verpoest, I.; Lomov, S. V. Voids in Fibre-Reinforced Polymer Composites: A Review on Their Formation, Characteristics, and Effects on Mechanical Performance. J. Compos. Mater. 2019, 53, 1579-1669. https://doi.org/10.1177/0021998318772152

[4] Rosemeier, M.; Lester, C.; Antoniou, A.; Fahrenson, C.; Manousides, N.; Balzani, C. Determination of As-Built Properties of Fibre Reinforced Polymers in a Wind Turbine Blade Using Scanning Electron and High-Resolution X-Ray Microscopy. Compos. Part C Open Access 2022, 9, 100310. https://doi.org/10.1016/j.jcomc.2022.100310

[5] Mallick, P.K. Fibre Reinforced Composites Material, Manufacturing, and Design; 2008; ISBN 9781119865544. https://doi.org/10.1201/9781420005981

[6] Parandoush, P.; Tucker, L.; Zhou, C.; Lin, D. Laser Assisted Additive Manufacturing of Continuous Fibre Reinforced Thermoplastic Composites. Mater. Des. 2017, 131, 186-195. https://doi.org/10.1016/j.matdes.2017.06.013

[7] Chung, H.; Das, S. Processing and Properties of Glass Bead Particulate-Filled Functionally Graded Nylon-11 Composites Produced by Selective Laser Sintering. Mater. Sci. Eng. A 2006, 437, 226-234. https://doi.org/10.1016/j.msea.2006.07.112

[8] Brøndsted, P.; Lilholt, H.; Lystrup, A. Composite Materials for Wind Power Turbine Blades. Annu. Rev. Mater. Res. 2005, 35, 505-538. https://doi.org/10.1146/annurev.matsci.35.100303.110641

[9] Kracalik, M.; Pospisil, L.; Slouf, M.; Mikesova, J.; Sikora, A.; Simonik, J.; Forteiny, I. Effect of Glass Fibres on Rheology, Thermal and Mechanical Properties of Recycled PET. Polym. Polym. Compos. 2008, 16, 101-113.

[10] Lee, N.J.; Jang, J. Effect of Fibre Content on the Mechanical Properties of Glass Fibre Mat/Polypropylene Composites. Compos. Part A Appl. Sci. Manuf. 1999, 30, 815-822. https://doi.org/10.1016/S1359-835X(98)00185-7

[11] Laura, D.M.; Keskkula, H.; Barlow, J.W.; Paul, D.R. Effect of Glass Fibre Surface Chemistry on the Mechanical Properties of Glass Fibre Reinforced, Rubber-Toughened Nylon 6. Polymer (Guildf). 2002, 43, 4673-4687. https://doi.org/10.1016/S0032-3861(02)00302-6

[12] Zhang, H.; Zhang, L.; Zhang, H.; Wu, J.; An, X.; Yang, D. Fibre Bridging and Nozzle Clogging in 3D Printing of Discontinuous Carbon Fibre-Reinforced Polymer Composites: Coupled CFD-DEM Modelling. Int. J. Adv. Manuf. Technol. 2021, 117, 3549-3562. https://doi.org/10.1007/s00170-021-07913-7

[13] Ramazani S. A., A.; Ait-Kadi, A.; Grmela, M. Rheology of Fibre Suspensions in Viscoelastic Media: Experiments and Model Predictions. J. Rheol. (N. Y. N. Y). 2001, 45, 945-962. https://doi.org/10.1122/1.1378026

[14] Huq, A.M.A.; Azaiez, J. Effects of Length Distribution on the Steady Shear Viscosity of Semiconcentrated Polymer-Fibre Suspensions. Polym. Eng. Sci. 2005, 45, 1357-1368. https://doi.org/10.1002/pen.20415

[15] Rashia Begum S., Vasumathi M., Karupaiah V., Narayanan, V (2024). Effect of process parameters on mechanical and tribological characteristics of FDM printed glass fiber reinforced PLA composites. Rapid Prototyping Journal, 30(9), 1859-1875. https://doi.org/10.1108/RPJ-03-2024-0121

[16] Iyer, S. S. G., & Keles, O. (2022). Effect of raster angle on mechanical properties of 3D printed short carbon fiber reinforced acrylonitrile butadiene styrene. Composites Communications, 32, 101163. https://doi.org/10.1016/j.coco.2022.101163

[17] Karad, A. S., Sonawwanay, P. D., Naik, M., & Thakur, D. G. (2023). Experimental study of effect of infill density on tensile and flexural strength of 3D printed parts. Journal of Engineering and Applied Science, 70(1), 104. https://doi.org/10.1186/s44147-023-00273-x

[18] Roy, R.; Mukhopadhyay, A. Tribological Studies of 3D Printed ABS and PLA Plastic Parts. Mater. Today Proc. 2021, 41, 856-862. https://doi.org/10.1016/j.matpr.2020.09.235

[19] Perepelkina, S.; Kovalenko, P.; Pechenko, R.; Makhmudova, K. Investigation of Friction Coefficient of Various Polymers Used in Rapid Prototyping Technologies with Different Settings of 3D Printing. Tribol. Ind. 2017, 39, 519-526. https://doi.org/10.24874/ti.2017.39.04.11

[20] Wang, X.; Jiang, M.; Zhou, Z.; Gou, J.; Hui, D. 3D Printing of Polymer Matrix Composites: A Review and Prospective. Compos. Part B Eng. 2017, 110, 442-458. https://doi.org/10.1016/j.compositesb.2016.11.034

[21] Mori, K.I.; Maeno, T.; Nakagawa, Y. Dieless Forming of Carbon Fibre Reinforced Plastic Parts Using 3D Printer. Procedia Eng. 2014, 81, 1595-1600. https://doi.org/10.1016/j.proeng.2014.10.196

[22] Baumann, F.; Scholz, J.; Fleischer, J. Investigation of a New Approach for Additively Manufactured Continuous Fibre-Reinforced Polymers. Procedia CIRP 2017, 66, 323-328. https://doi.org/10.1016/j.procir.2017.03.276

[23] Franco-Urquiza, E.A.; Escamilla, Y.R.; Llanas, P.I.A. Characterization of 3D Printing on Jute Fabrics. Polym. 2021,

Vol. 13, Page 3202 2021, 13, 3202. https://doi.org/10.3390/polym13193202

[24] Ismail, K.I.; Ramarad, S.; Yap, T.C. Design and Fabrication of an In Situ Short-Fibre Doser for Fused Filament Fabrication 3D Printer: A Novel Method to Manufacture Fibre-Polymer Composite. Inventions 2023, 8. https://doi.org/10.3390/inventions8010010

[25] Ismail, K.I.; Pang, R.; Ahmed, R.; Yap, T.C. Tensile Properties of In Situ 3D Printed Glass Fibre-Reinforced PLA. Polym. 2023, Vol. 15, Page 3436 2023, 15, 3436. https://doi.org/10.3390/polym15163436

[26] Hasan, M.R.; Davies, I.J.; Pramanik, A.; John, M.; Biswas, W.K. Impact of Process Parameters on Improving the Performance of 3D Printed Recycled Polylactic Acid (RPLA) Components. Int. J. Adv. Manuf. Technol. 2024, 131, 3751-3779. https://doi.org/10.1007/s00170-024-13140-7

[27] Slapnik, J.; Bobovnik, R.; Mešl, M.; Bolka, S. Modified Polyactide Filaments for 3D Printing with Improved Mechanical Properties. Contemp. Mater. 2016, 7, 142-150. https://doi.org/10.7251/COMEN1602142S

[28] Laureto, J.; Tomasi, J.; King, J.A.; Pearce, J.M. Thermal Properties of 3-D Printed Polylactic Acid-Metal Composites. Prog. Addit. Manuf. 2017, 2, 57-71. https://doi.org/10.1007/s40964-017-0019-x

[29] Andrew, J.J.; Schneider, J.; Ubaid, J.; Velmurugan, R.; Gupta, N.K.; Kumar, S. Energy Absorption Characteristics of Additively Manufactured Plate-Lattices under Low- Velocity Impact Loading. Int. J. Impact Eng. 2021, 149, 103768. https://doi.org/10.1016/j.ijimpeng.2020.103768

[30] Nam, R.; Jakubinek, M.; Niknam, H.; Rahmat, M.; Ashrafi, B.; Naguib, H.E. 3D Printed Octet Plate-Lattices for Tunable Energy Absorption. Mater. Des. 2023, 228, 111835. https://doi.org/10.1016/j.matdes.2023.111835

[31] Ho, M.P.; Lau, K.T. Enhancement of Impact Resistance of Biodegradable Polymer Using Bamboo Charcoal Particles. Mater. Lett. 2014, 136, 122-125. https://doi.org/10.1016/j.matlet.2014.07.165

[32] Mohankumar, H.R.; Benal, M.G.M.; Pradeepkumar, G.S.; Tambrallimath, V.; Ramaiah, K.; Khan, T.M.Y.; Bhutto, J.K.; Ali, M.A. Effect of Short Glass Fibre Addition on Flexural and Impact Behavior of 3D Printed Polymer Composites. ACS Omega 2023, 8, 9212-9220. https://doi.org/10.1021/acsomega.2c07227

[33] Aslan, M.; Kaya, M.; Güler, O.; Alver, Ü.; Teknik Üniversitesi, K.; ve Malzeme Mühendisliği Bölümü, M.; Kampüsü, K. Effect of Fibre Content on the Mechanical Properties of Basalt Fibre Reinforced Polyactic Acid (PLA) Composites. Text. Appar. 2018, 28, 66-71.

[34] El-Sayed, A.A.; El-Sherbiny, M.G.; Abo-El-Ezz, A.S.; Aggag, G.A. Friction and Wear Properties of Polymeric Composite Materials for Bearing Applications. Wear 1995, 184, 45-53. https://doi.org/10.1016/0043-1648(94)06546-2

[35] Yetistiren, H.; Zeren, A.; Tülin Şahin Wear Properties of Glass Fibre Reinforced Polypropylene. KGK rubberpoint 2012, 65, 43-48.

[36] Striemann, P.; Bulach, S.; Hülsbusch, D.; Niedermeier, M.; Walther, F. Shear Characterization of Additively Manufactured Short Carbon Fibre-Reinforced Polymer. Macromol. Symp. 2021, 395, 2000247. https://doi.org/10.1002/masy.202000247

[37] Kuncius, T.; Rimašauskas, M.; Rimašauskienė, R. Interlayer Adhesion Analysis of 3D-Printed Continuous Carbon Fibre-Reinforced Composites. Polym. 2021, Vol. 13, Page 1653 2021, 13, 1653. https://doi.org/10.3390/polym13101653

[38] Radzuan, N.A.M.; Sulong, A.B.; Verma, A.; Muhamad, N. Layup Sequence and Interfacial Bonding of Additively Manufactured Polymeric Composite: A Brief Review. Nanotechnol. Rev. 2021, 10, 1853-1872. https://doi.org/10.1515/ntrev-2021-0116

[39] Chand, N.; Naik, A.; Neogi, S. Three-Body Abrasive Wear of Short Glass Fibre Polyester Composite. Wear 2000, 242, 38-46. https://doi.org/10.1016/S0043-1648(00)00398-7

https://doi.org/10.12974/2311-8717.2026.14.07